tvst

Article

Microscope-integrated Intraoperative Optical Coherence Tomography for Anterior Segment Surgical Maneuvers

Wangyi Fang[1,2,*], Qingchen Li[1,2,*], Jinyu Fan[3], Ning Tang[3], Jian Yu[1,2], Huan Xu[1,2], Yuan Zong[1,2], Chunhui Jiang[1,2], Guohua Shi[3], and Xinghuai Sun[1,2]

[1] Department of Ophthalmology and Vision Science, Eye and ENT Hospital, Fudan University, Shanghai, 200031, People's Republic of China
[2] Key Laboratory of Myopia of State Health Ministry, and Key Laboratory of Visual Impairment and Restoration of Shanghai, Shanghai, 200031, People's Republic of China
[3] Suzhou Institute of Biomedical Engineering and Technology, Chinese Academy of Sciences, Suzhou, Jiangsu Province, China

Correspondence: Chunhui Jiang, Department of Ophthalmology and Vision Science, Eye and ENT Hospital, Fudan University, 83 Fenyang Rd, Shanghai 200031, People's Republic of China. e-mail: chhjiang70@163.com
Guohua Shi, Jiangsu Key Laboratory of Medical Optics, Suzhou Institute of Biomedical Engineering and Technology, Chinese Academy of Sciences, 88 Kelin Rd, Suzhou 215163, People's Republic of China; CAS Center for Excellence in Brain Science and Intelligence Technology, Shanghai 200031, China. e-mail: ghshi_lab@126.com

Received: December 13, 2019
Accepted: April 21, 2020
Published: June 18, 2020

Keywords: swept-source optical coherence tomography; microscope integrated; intraoperative; surgical maneuvers; surgical training

Citation: Fang W, Li Q, Fan J, Tang N, Yu J, Xu H, Zong Y, Jiang C, Shi G, Sun X. Microscope-integrated intraoperative optical coherence tomography for anterior segment surgical maneuvers. Trans Vis Sci Tech. 2020;9(7):18, https://doi.org/10.1167/tvst.9.7.18

Purpose: To evaluate the potential value of microscope-integrated optical coherence tomography (MI-OCT) in anterior segment surgical maneuvers.

Methods: Twenty-four ophthalmology residents, who were randomly and evenly divided into two groups, performed four anterior segment surgical maneuvers (corneal tunnel, scleral tunnel, simple corneal suture, and corneal laceration repair) on porcine eyes with (group B) or without (group A) real-time MI-OCT feedback. All residents performed the maneuvers again without MI-OCT.

Results: Compared with group A, group B (with MI-OCT) showed better accuracy in the length/depth of the corneal tunnel and the length of the scleral tunnel. However, both groups showed similar performances in the depth of both the simple corneal suture and the corneal laceration suture. When both groups performed the maneuvers again without MI-OCT, group B still showed better results than group A for the length of both the corneal and scleral tunnels.

Conclusions: Primary results suggest that real-time MI-OCT images are valuable for some anterior segment surgical maneuvers and could be helpful in surgical training.

Translational Relevance: MI-OCT systems can be valuable in improving accuracy and decision making during anterior segment surgery and will be useful in surgical training.

Introduction

After its introduction in 1876, the microscope has greatly improved ocular surgical treatment through magnification of the surgical view.[1] Despite ongoing development, the microscope has remained limited in that it only provides information on an en face level. In contrast, optical coherence tomography (OCT), which was introduced into the field of

ophthalmology by Huang et al. in 1991,[2] is able to provide tissue-level high-resolution tomographic information in a noncontact way and has revolutionized our understanding of many eye entities. If a combination of en face and tomographic information could be provided simultaneously to the surgeon, this may have a positive impact on the surgical treatment of ocular diseases. Many researchers have attempted this maneuver; however, early studies involving intraoperative OCT imaging reported that the surgery had to be stopped and in some cases the microscope had to be removed.[3–10] These findings placed doubt on the potential clinical value of this combined system.

Owing to the recent developments in surgical technique and engineering, microscope-integrated OCT (MI-OCT) systems have been developed.[11] Early trials have indicated that MI-OCT is helpful in both retinal and anterior segment surgeries.[8–9,12–17] However, most systems use a wavelength of 840 nm that is designed for guidance during vitreoretinal surgery and ideal for fundus imaging. Anterior segment OCT, which adopts a light source with a wavelength of 1310 nm, has been used in the clinic for a long time. Here, using a tailor-made MI-OCT system with a wavelength of 1310 nm, we aimed to evaluate the potential value of MI-OCT in anterior segment surgical maneuvers.

Methods

This study was approved by the Institutional Review Board of the Eye and ENT Hospital of Fudan University, Shanghai, China (No. 2019031-1).

Participants and Surgical Maneuver Procedures

A group of 24 ophthalmology residents with similar surgical experience were included and were randomly divided into two equal groups (group A and group B). The randomization was conducted using a random number generator and the sort cases function of the SPSS software (SPSS Inc., Chicago, IL).

Residents were asked to perform four basic ophthalmic surgical maneuvers[18–20] on freshly enucleated porcine eyes: (1) creating a 2-mm length clear corneal tunnel at 50% depth, (2) creating a 2-mm length scleral tunnel at 50% depth, (3) simple corneal suturing (SCS) at 90% depth, and (4) repairing a full-thickness corneal laceration repair (CLR) at 90% depth. The corneal and scleral tunnels were made using a 2.8-mm artificial sapphire knife, and the sutures were performed with 10-0 nylon sutures (Ethicon, Somerville, NJ). All residents watched the same set of PowerPoint slides introducing the four surgical maneuvers and the MI-OCT system (Fig. 1). To eliminate the influence of the learning curve, surgeons were asked to repeat the surgical maneuvers six times using the same system (without OCT feedback) before the study.

In the study, two consecutive trials were performed. In trial one, all residents performed the same four surgical maneuvers, without MI-OCT feedback in group A and with MI-OCT feedback in group B. In trial two, the same four maneuvers were repeated by both groups without MI-OCT feedback (Supplementary Fig. S1). In trials one and two, for each resident, every maneuver was performed on a new porcine eye, so in total 192 porcine eyes were used. The OCT images were only displayed to group B in trial one, but the light of the diode, which indicates the region of OCT scanning, was visible to all participants; therefore, OCT images of the proper area could be seen by a second operator who monitored and recorded the OCT images at the end of the maneuver for later measurement.

MI-OCT, Imaging, and Measurement

Swept-source OCT was optically designed to work in conjunction with the optical path of the microscope in the prototype MI-OCT, both sharing an objective lens with a 200-mm focal length. Swept-source OCT operates in the 1310-nm wavelength range at a high axial scan rate of 100 kHz, with a high-speed tunable laser (HSL-20, Santec, Aichi, Japan). The lateral resolution was 14 μm, and the lateral range was 10.7 mm with a 768 A-scan/B-scan. The axial resolution and the maximum depth in the air were 11 μm and 6 mm, respectively. After detection, OCT signals were processed with a high-performance computer (CPU: E5-2620v4@2.1 GHz, RAM: 32 GB, graphics cards: GTX1080Ti), and real-time OCT images were output. A super luminescent diode with a wavelength of 640 nm was combined in a sample arm of the OCT and used to mark the OCT scanning region. Binocular microscopic images were separated by a beam splitter and recorded by two surgical video cameras (MCC-500MDC, SONY, Tokyo, Japan) and subsequently displayed on an HD (1080P, 1920×1080) 42-inch widescreen LCD 3D monitor (LMD-4251TD, SONY) with/without the OCT real-time image. Residents were required to wear circular polarizer three-dimensional (3D) glasses that give precise depth perception. The final time delay of OCT images and dual channel microscopic images were less than 120 ms and 100 ms, respectively.

OCT images were taken at the end of the maneuver by a second operator and stored for later measurement.

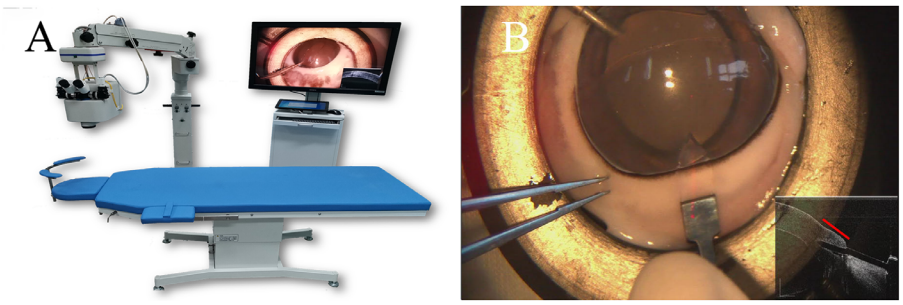

Figure 1. The MI-OCT system. (A) Laboratory setup: the MI-OCT system and head-up display screen. (B) Image projected on the screen: the image from the microscope and the OCT (lower left corner, only displayed to group B in trial one). The *red line* in the microscope image indicates the OCT scanning beam, and the *red line* on the OCT image indicates the 2-mm length (only displayed to group B in trial one).

For the corneal and scleral tunnel, B-scans perpendicular to the limbus and crossing the center of the tunnel were taken. In the prestudy experiment, it was found, that after withdrawal of the knife, the end of the scleral tunnel was not clear; as a result, a piece of 0.10-mm thick polyvinyl chloride film was inserted into the incision while the images were taken to ensure an accurate measurement. For SCS and full thickness CLR, images were taken in the same direction as the suture.

Image readers were blinded to the type of image they were assessing using Photoshop (Adobe Systems Corporation, San Jose, CA). Two readers with good consistency (Supplementary Table S1) performed the measurement separately, and the average was used for final analysis. The lengths of the corneal and scleral tunnels were measured from the start of the horizontal part to the end. The depth of the corneal tunnel was measured at the end of the tunnel: the shortest distance from the epithelium of the corneal to the end of the tunnel. This distance was subsequently divided by the shortest distance of the linear path between the endothelium and epithelium at the same location, and this percentage was used for further analysis. For scleral tunnel depth, the inner boundary of the sclera was not clear in many of the cases, so the measurement was not performed (Supplementary Fig. S2). For SCS, the depth of the suture was measured as the shortest distance from the epithelium of the corneal to the lowest point of the suture. This distance was subsequently divided by the shortest distance of the linear path between the endothelium and epithelium at the same location, and this percentage was used for further analysis. For corneal laceration sutures, the depth was the shortest distance from the epithelial of the cornea to the suture at the location of the laceration (white solid line). This distance was subsequently divided by the shortest distance of the linear path between the endothelium and epithelium at the same location, and this percentage was used for further analysis.

Statistics

All statistics are presented as mean ± standard deviation. Absolute values of the deviation between the actual measured values and the target values were used for analysis. The statistical comparisons conducted across group A and group B were performed by independent sample t tests, and the Welch's t test was used for unequal variances, including the corneal tunnel length and depth deviation in both trials and the scleral tunnel length deviation in trial two. The comparison between the performance of group B in trial one and trial two was performed using the paired samples t test. P values of less than 0.05 were deemed statistically significant.

Results

Trial One

The average length and depth of the corneal tunnel was 2.67 ± 0.47 mm and 57.39 ± 18.67%, respectively, in group A and 2.08 ± 0.12 mm and 52.31 ± 4.57%, respectively, in group B. Group B showed better accuracy in both length and depth than did group A (absolute deviation length: group A 0.71 ± 0.41 mm vs. group B 0.09 ± 0.11 mm; $P = 0.003$; deviation depth: group A 14.35 ± 13.54% vs. group B 3.9 ± 3.05%; $P = 0.024$) (Fig. 2). The average length of the scleral tunnel was 2.34 ± 0.60 mm in group A and 2.03 ± 0.15 mm in group B, and this difference was statistically significant (deviation: group A 0.49 ± 0.47 mm vs. group B 0.11 ± 0.10 mm; $P = 0.008$) (Fig. 3).

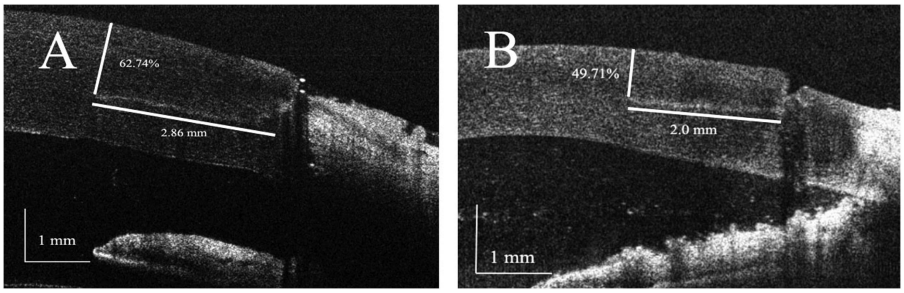

Figure 2. Representative OCT images of corneal tunnel from group A (A) and group B (B) in trial one.

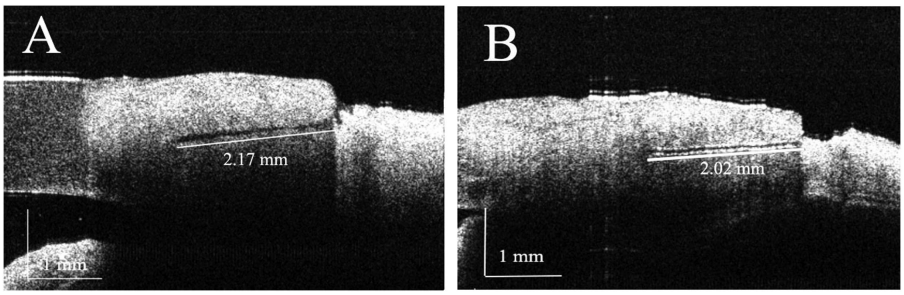

Figure 3. Representative OCT images of scleral tunnel from group A (A) and group B (B) in trial one.

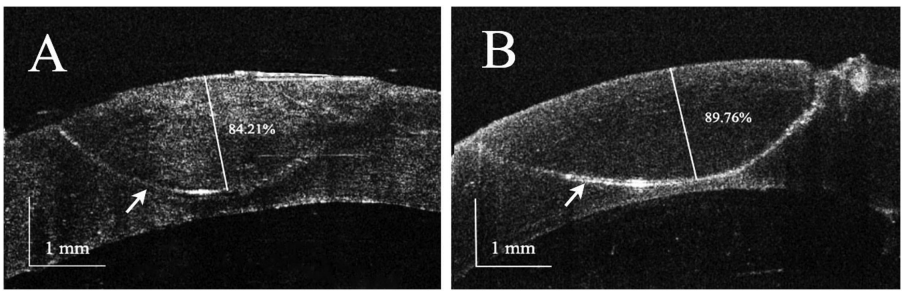

Figure 4. Representative OCT images of the simple corneal suture from group A (A) and group B (B). The linear hyper-reflective signal in the cornea is the 10-0 polyamide suture (*white arrows*). Depth of the suture was presented in percentage.

For SCS and CLR, the average suture depths were 82.02 ± 10.66% and 73.76 ± 8.42%, respectively, in group A and 83.80 ± 9.18% and 76.82 ± 7.18%, respectively, in group B. The two groups showed similar performances (deviation SCS: group A 11.208 ± 6.79% vs. group B 8.94 ± 6.24%; $P = 0.405$; CLR: group A 16.24 ± 8.42% vs. group B 13.18 ± 7.18%; $P = 0.348$) (Figs. 4 and 5, Supplementary Fig. S3).

Trial Two

When the two groups performed the maneuvers again without OCT feedback, group B still showed a better accuracy in the length of the corneal tunnel and the scleral tunnel than did group A (deviation of the corneal tunnel length: group A 0.53 ± 0.37 mm vs. group B 0.17 ± 0.09 mm; $P = 0.006$; deviation of the scleral tunnel length: group A 0.49 ± 0.60 mm vs. group B 0.12 ± 0.10 mm; $P = 0.020$); the performances for all other maneuvers were similar (all $P > 0.05$) (Table, Supplementary Fig. S3).

Discussion

In this prospective randomized study, the value of using MI-OCT during anterior segment surgical maneuvers was evaluated. The results suggested that MI-OCT was able to provide high-resolution real-time images of the anterior segment, and these images helped the surgeon to make important

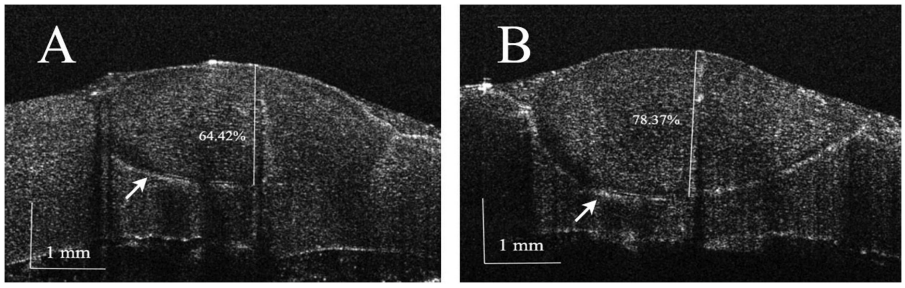

Figure 5. Representative OCT images of CLR from group A (A) and group B (B). The linear hyper-reflective signal in the cornea is the 10-0 polyamide suture (*white arrows*). Depth of the suture was presented in percentage.

Table. Comparison of the Deviations Between Groups A and B

		Corneal Tunnel		Scleral Tunnel	Simple Corneal Suture	Corneal Laceration Suture
	P Value	Length	Depth	Length	Depth	Depth
Trial 1	A vs. B	0.003*	0.024*	0.008*	0.405	0.348
Trial 2	A vs. B	0.006*	0.092	0.020*	0.134	0.621
Trial 1/2	B vs. B	0.505	0.666	0.168	0.695	0.347

For each resident, every maneuver was performed on a new porcine eye. The values in all columns are absolute values of the deviation between the actual measured value and the target value. Group A = without MI-OCT and group B = with MI-OCT.
*Statistically significant difference.

intraoperative decisions and improve the surgical outcomes of select anterior segment maneuvers. Furthermore, the technique acquired with MI-OCT persisted when residents performed the maneuvers again without OCT feedback.

Recently, intraoperative OCT has been used to monitor and guide ocular surgery and been found useful during both anterior and posterior ocular surgeries.[8–17] However, certain limitations have been noted, including the use of an external display of the OCT image, which means that the surgeon has to move away from the oculars of the microscope to look at the OCT images on the external screen. Some researchers have reported that the use of an external display for the OCT image decreases the value of MI-OCT.[19] An alternative way is to project the image within the ocular.[7] However, this strategy limits the resolution of the projected image.[7,21]

To the best of our knowledge, our system is the first MI-OCT system that projects high-resolution OCT images and 3D surgical images simultaneously on the same screen. Live 3D surgery, which was first reported by Weinstock in 2008, has been reported as helpful during ocular surgery.[22–24] In this study, by projecting the high-resolution images from the two systems simultaneously and side by side, the surgeon was able to use the information provided by the OCT throughout the whole surgery. Furthermore, although use of a 3D viewing system is not a daily occurrence for most surgeons, the learning curve required was short.[25,26]

Our results suggest that real-time, tissue-level, high-resolution images provided by the OCT help the surgeon to make decisions, especially during length-based maneuvers (2-mm corneal and 2-mm scleral tunnel). During the maneuver, a line corresponding to 2 mm in length at the tissue level was projected on the screen; therefore, it was quite easy for the surgeon to stop at the ideal point. We showed that the deviation of length was 0.09 ± 0.11 mm for the corneal tunnel and 0.03 ± 0.09 mm for the scleral tunnel when OCT feedback was used and 0.71 ± 0.41 mm and 0.18 ± 0.55 mm, respectively, when it was not. The MI-OCT also improved corneal thickness outcomes with a deviation of corneal tunnel thickness of 3.9 ± 3.05% when OCT feedback was used and 14.35 ± 13.54% when it was not. In a previous report, Todorich et al.[19] reported that MI-OCT feedback was not helpful for making corneal incisions, and they thought that this might be associated with the complete shadowing of the underlying structure by the metal keratome (which was also noticed in our study; Supplementary Fig. S4) and the use of an external OCT image display. In contrast, apart from the concomitant display of the OCT image and 3D microscope images, an artificial

sapphire knife was also used. During the procedure, the tissue beneath the knife could be clearly visualized; therefore, the difference in the system and instrument used might contribute to the different findings of the two studies.

Our results also indicated that OCT was not helpful for all surgical maneuvers. In suture maneuvers, the group with OCT feedback showed similar performance to the group without it (all $P > 0.05$). Combined with the feedback from the surgeons, we anticipated that the reasons might be that, during the suturing, the corneal tissue was twisted and torqued, the metal forceps shadowed the underlying tissue, and it was very difficult to assess the exact position of the needle in the corneal tissue, especially in CLRs. The position of the needle could be fully appreciated after the needle had been placed and the forceps removed, but it was too late at the time. In the study by Todorich et al.,[19] they found that MI-OCT helped in corneal suturing; however, in their study, the surgeons could remove the needle and try again based on MI-OCT feedback and the surgeons had three chances to place the suture in the right position, whereas in our study, the surgeons had only one chance. This difference in the process might account for the difference in the results of the two studies.

In trial two, when group B performed the maneuvers without OCT feedback, they still achieved less deviation than did group A for corneal and scleral tunnel length (all $P < 0.05$). Furthermore, the results were comparable to their own results from trial one with MI-OCT feedback (Table, Supplementary Fig. S3). This finding was in accordance with the findings of Todorich et al., in which MI-OCT led to sustained learning of surgical skills, and better results were seen even when MI-OCT feedback was not subsequently available.[19] Their study, as well as ours, indicates that MI-OCT is valuable in the training of surgical techniques. However, we must not forget the limitations of the system, namely, the lack of a tracking system and the fact that the surgeons needed to stop the maneuver and move the OCT scan beam to the region of interest. Furthermore, specially designed OCT-friendly surgical instruments need to be developed in the future. Also, our study was performed on porcine eyes and only residents participated.

In conclusion, the MI-OCT system used in this study was able to provide real-time, high-resolution OCT images during the whole procedure, and these images helped the residents to make important decisions and improved the outcomes of select surgical maneuvers. Much work is still required to improve the system and to find the optimal way to use the MI-OCT system in clinic practice.

Acknowledgments

Supported, in part, by research grants from the National Key Research & Development Plan (2017YFC0108200, 2017YFC0108201), the Shanghai Committee of Science and Technology (19441900900), Jiangsu Province Key Research & Development Program (BE2018667).

Disclosure: **W. Fang**, None; **Q. Li**, None; **J. Fan**, None; **N. Tang**, None; **J. Yu**, None; **H. Xu**, None; **Y. Zong**, None; **C. Jiang**, None; **G. Shi**, None; **X. Sun**, None

* WF and QL contributed equally to this study and share first authorship.

References

1. Barraquer JI. The history of the microscope in ocular surgery. *J Microsurg*. 1980;1:288–299.
2. Huang D, Wang J, Lin CP, Puliafito CA, Fujimoto JG. Micron-resolution ranging of cornea anterior chamber by optical reflectometry. *Lasers Surg Med*. 1991;11:419–425.
3. Binder S, Falkner-Radler CI, Hauger C, Matz H, Glittenberg C. Feasibility of intrasurgical spectral-domain optical coherence tomography. *Retina*. 2011;31:1332–1336.
4. Hahn P, Migacz J, O'Connell R, Maldonado RS, Izatt JA, Toth CA. The use of optical coherence tomography in intraoperative ophthalmic imaging. *Ophthalmic Surg Lasers Imaging*. 2011;42:S85–94.
5. Ray R, Baranano DE, Fortun JA, et al. Intraoperative microscope-mounted spectral domain optical coherence tomography for evaluation of retinal anatomy during macular surgery. *Ophthalmology*. 2011;118:2212–2217.
6. Pichi F, Alkabes M, Nucci P, Ciardella AP. Intraoperative SD-OCT in macular surgery. *Ophthalmic Surg Lasers Imaging*. 2012;43:S54–S60.
7. Ehlers JP, Goshe J, Dupps WJ, et al. Determination of feasibility and utility of microscope-integrated optical coherence tomography during ophthalmic surgery: the DISCOVER Study RESCAN results. *JAMA Ophthalmol*. 2015;133:1124–1132.
8. Ehlers JP, Ohr MP, Kaiser PK, Srivastava SK. Novel microarchitectural dynamics in rhegmatogenous retinal detachments identified with

intraoperative optical coherence tomography. *Retina*. 2013;33:1428–1434.
9. Ehlers JP, Tam T, Kaiser PK, Martin DF, Smith GM, Srivastava SK. Utility of intraoperative optical coherence tomography during vitrectomy surgery for vitreomacular traction syndrome. *Retina*. 2014;34:1341–1346.
10. Dayani PN, Maldonado R, Farsiu S, Toth CA. Intraoperative use of handheld spectral domain optical coherence tomography imaging in macular surgery. *Retina*. 2009;29:1457–1468.
11. Carrasco-Zevallos OM, Viehland C, Keller B, et al. Review of intraoperative optical coherence tomography: technology and applications [Invited]. *Biomed Opt Express*. 2017;8:1607–1637.
12. Huttmann G, Lankenau E, Schulz-Wackerbarth C, Muller M, Steven P, Birngruber R. [Optical coherence tomography: from retina imaging to intraoperative use - a review]. *Klin Monbl Augenheilkd*. 2009;226:958–964.
13. Pasricha ND, Shieh C, Carrasco-Zevallos OM, et al. Real-time microscope-integrated OCT to improve visualization in DSAEK for advanced bullous keratopathy. *Cornea*. 2015;34:1606–1610.
14. Pasricha ND, Shieh C, Carrasco-Zevallos OM, et al. Needle depth and big-bubble success in deep anterior lamellar keratoplasty: an ex vivo microscope-integrated OCT study. *Cornea*. 2016;35:1471–1477.
15. Falkner-Radler CI, Glittenberg C, Gabriel M, Binder S. Intrasurgical microscope-integrated spectral domain optical coherence tomography-assisted membrane peeling. *Retina*. 2015;35:2100–2106.
16. De Benito-Llopis L, Mehta JS, Angunawela RI, Ang M, Tan DT. Intraoperative anterior segment optical coherence tomography: a novel assessment tool during deep anterior lamellar keratoplasty. *Am J Ophthalmol*. 2014;157:334–341.
17. Steven P, Le Blanc C, Velten K, et al. Optimizing Descemet membrane endothelial keratoplasty using intraoperative optical coherence tomography. *JAMA Ophthalmol*. 2013;131:1135–1142.
18. Hayashi K, Tsuru T, Yoshida M, Hirata A. Intraocular pressure and wound status in eyes immediately after scleral tunnel incision and clear corneal incision cataract surgery. *Am J Ophthalmol*. 2014;158:232–241.
19. Todorich B, Shieh C, DeSouza PJ, et al. Impact of microscope-integrated OCT on ophthalmology resident performance of anterior segment surgical maneuvers in model eyes. *Invest Ophthalmol Vis Sci*. 2016;57:OCT146–153.
20. Marian SM. *Ophthalmic microsurgical suturing techniques*. Berlin, Heidelberg: Springer-Verlag; 2007:49–60.
21. Pahuja N, Shetty R, Jayadev C, Nuijts R, Hedge B, Arora V. Intraoperative optical coherence tomography using the RESCAN 700: preliminary results in collagen crosslinking. *Biomed Res Int*. 2015;2015:572698.
22. Weinstock RJ, Desai N. Heads-up cataract surgery with the TrueVision 3D Display System. In: Garg A, Alio JL, Eds. *Surgical techniques in ophthalmology. Cataract surgery*. New Delhi, India: 2010, pp. 124–127.
23. Weinstock RJ. Operate with your head up. *Cataract Refract Surg Today*. 2011;8:66–74.
24. Eckardt C, Paulo EB. Heads-up surgery for vitreoretinal procedures: an experimental and clinical study. *Retina*. 2016;36:137–147.
25. Palacios RM, Maia A, Farah ME, Maia M. Learning curve of three-dimensional heads-up vitreoretinal surgery for treating macular holes: a prospective study. *Int Ophthalmol*. 2019;39:2353–2359.
26. Zhang T, Tang W, Xu G. Comparative analysis of three-dimensional heads-up vitrectomy and traditional microscopic vitrectomy for vitreoretinal diseases. *Curr Eye Res*. 2019;44:1080–1086.